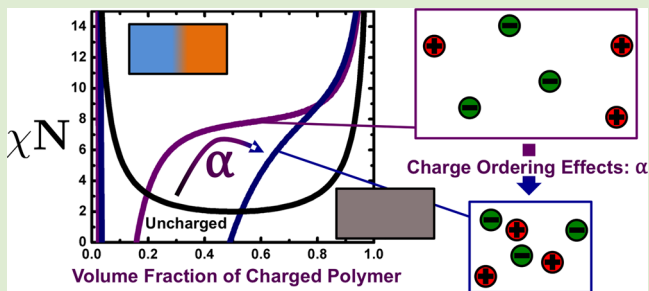


# Polyelectrolyte Blends and Nontrivial Behavior in Effective Flory–Huggins Parameters

Charles E. Sing and Monica Olvera de la Cruz\*

Department of Materials Science and Engineering, Northwestern University, Evanston, Illinois 60208, United States

**ABSTRACT:** The Flory  $\chi$ -parameter is a ubiquitous description of the extent of immiscibility that is apparent between two or more polymeric species. While the formalism is a powerful one in most systems of technological interest, experimentally obtaining this parameter requires the assumption of an underlying theoretical model. For charged systems, mapping to analogous uncharged systems is often assumed by introducing an “effective  $\chi$ ”,  $\chi_{\text{eff}}$ . Random phase approximation (RPA) analysis based on the Hamiltonian used for recent self-consistent field theory–liquid-state theories (SCFT–LS) demonstrates that  $\chi_{\text{eff}}$  incorporates molecular-level details such as charge ordering. Even for simple polyelectrolyte blends where the bare  $\chi$  is kept constant, the observed  $\chi_{\text{eff}}$  will drastically change as a function of composition; prediction of heterogeneous polyelectrolyte material phase behavior using  $\chi_{\text{eff}}$  is thus highly nontrivial since an understanding of local charge structure is required.



Complex polymer systems involving more than one species are almost overwhelmingly described both conceptually and mathematically by the language that Flory and Huggins laid down more than half a century ago.<sup>1–3</sup> The simplicity of the model harkens back to even older ideas regarding solution models used to describe miscibility in multicomponent liquids, such as regular solution theory,<sup>3</sup> and is therefore a powerful formalism that is often useful. In Flory–Huggins theory, the  $\chi$ -parameter was introduced to represent the enthalpic contributions to the mixing free energy and physically represents the energy penalty in  $k_B T$  that arises due to the short-ranged (typically dispersive) interactions between two spatially adjacent components.<sup>2</sup> More advanced theories typically adopt the  $\chi$ -parameter formalism in the creation of their models due to its clear interpretation.<sup>4,5</sup> Accordingly, experimental methods rely on these theoretical models to interpret scattering data as a way to *measure* the value of  $\chi$  in multicomponent polymer systems.<sup>5–7</sup>

Work on polyelectrolyte blends and block copolymers has adopted this formalism; in particular, an “effective  $\chi$ ” ( $\chi_{\text{eff}}$ ) has been invoked to examine the phase behavior of these systems.<sup>7–11</sup> While such a method of characterizing a heterogeneous polyelectrolyte melt system is practical and conceptually appealing, the use of a  $\chi_{\text{eff}}$  in charged systems often leads to difficulty when interpreting the physical reasons for these parameters since the  $\chi_{\text{eff}}$  is no longer simply a description of local dispersive interactions but rather includes complicated charge effects. In particular, while many reports on limited regions of the otherwise expansive parameter space governing heterogeneous polyelectrolyte systems (e.g., charge fraction, bare  $\chi$ -parameter, composition, dielectric constant, etc.) lead to straightforward trends such as linear corrections to  $\chi$  proportional to the charge fraction,<sup>9–11</sup> such approaches do

not always hold when larger parameter spaces are considered.<sup>12,13</sup> We seek a general result that links the behavior of charges on a molecular level to measured values of  $\chi_{\text{eff}}$ .

Recent advances in understanding heterogeneous polyelectrolyte systems in the melt state have relied upon the development of multiscale theoretical calculations that simultaneously articulate polymer length-scale architectures and ion-scale charge ordering effects.<sup>14,15</sup> These tools have been applied to a number of practical material problems, in particular the cases of polyelectrolyte blends<sup>14,15</sup> and block copolyelectrolytes;<sup>16</sup> these investigations have demonstrated phase behaviors that are vastly different from those predicted by more traditional approaches yet have so far been able to explain many of the surprising results in the experimental literature.<sup>15,16</sup> For low dielectric constant media, simulations and theory demonstrate that strong Coulombic interactions between backbone charges and counterions result in the formation of local ordering.<sup>14,17</sup> This typically results in highly asymmetric phase diagrams, which are highly distorted from analogous uncharged polymer systems.<sup>14,15</sup> It is therefore apparent that the  $\chi_{\text{eff}}$  formalism is dubious since a straightforward mapping between the charged and uncharged systems is not trivial; we can use standard random phase approximation (RPA) analysis to demonstrate that even for the highly simplified case of a polyelectrolyte blend such a mapping requires knowledge of the local structure.

RPA analysis can characterize the concentration fluctuations around (for example) a homogeneous disordered state and can determine both scattering functions  $S(k)$  and regimes of

Received: April 4, 2014

Accepted: July 3, 2014

Published: July 9, 2014

thermodynamic stability for mixtures upon assuming perturbations up to second order.<sup>5,18</sup> The validity of this type of analysis can be interrogated by systematically introducing terms of higher order, which are often required for complicated systems such as block copolymers to correctly describe a system's critical properties.<sup>5,19,20</sup> Use of RPA in polyelectrolyte systems has a long history of development.<sup>21–26</sup> Most works consider a Hamiltonian that directly includes an electrostatic energy term and an ion entropy term via a potential field that becomes the electrostatic potential upon extremization of the overall Hamiltonian.<sup>4,24,25,27</sup> While this Hamiltonian itself is essentially exact, the introduction of perturbation approaches such as RPA is known to be insufficient for charged systems even when higher-order terms are included.<sup>27</sup> The origin of this complication is due to the long-range charge interactions, which do not tend to converge in perturbation treatments.<sup>27</sup>

A new version of this Hamiltonian  $\tilde{\mathcal{H}}_{\text{RPA-LS}}$  has recently been developed to overcome these difficulties and has been previously used in the development of hybrid self-consistent field theory–liquid-state (SCFT–LS) methods.<sup>14</sup> While the SCFT calculation is inherently a mean-field approach, we self-consistently incorporate information from LS theory that is beyond mean-field to circumvent the issues with treating a charged system using perturbative approaches.<sup>14,27</sup> The system we will consider is a polyelectrolyte blend, whose components are a charged polymer A and an uncharged polymer B (see Figure 1). The volume fraction of each component is  $\phi_A$  and

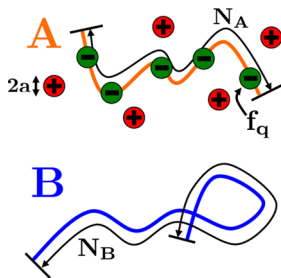


**Figure 1.** Schematic of the species in a polyelectrolyte blend; A and B are polymeric species. For the purposes of this paper, A will have a fraction  $f_q$  of monomers that are negatively charged. Each of these charges has a corresponding counterion that has a positive charge. Structure at the local charge-ordering level considers positive and negative charges to have radii of  $a$ . B will remain uncharged. A and B have lengths of  $N_A$  and  $N_B$  monomers, respectively; for this paper  $N_A = N_B = N = 40$ . These polymers have a short-range interaction  $\chi$ , which does not consider charge effects.  $\chi_{\text{eff}}$  attempts to incorporate charge effects into a related parameter.

$\phi_B$  for A and B, respectively. A has a length of  $N_A$  monomers, with a fraction  $f_q$  that have a negative charge, and B has a length of  $N_B$  monomers ( $N_A = N_B = N$  for this manuscript). Monomers have a volume  $\nu_0$ . Each negative charge has a corresponding positive counterion, and both have a radius  $a$ . The electrostatic interaction strength between the charged species is parametrized by  $\Gamma = e^2/(8\pi\epsilon_r\epsilon_0ak_B T)$ , which is the contact energy in units of  $k_B T$  between two like-charged species. This is a function of relative dielectric constant  $\epsilon_r$  and  $a$ ; a value of  $\Gamma \approx 1$  corresponds to charge interactions in aqueous, monovalent solutions; however, for polymer melts  $\Gamma \approx 10$ – $50$ . This range results from considering charges with  $a \approx 0.25$ – $0.3$  nm in a polymer with  $\epsilon_r \approx 4$ – $8$ , which are typical literature values.<sup>10</sup> For this work we focus on the situation that

$\epsilon_{r,A} = \epsilon_{r,B}$ ; however, there are well-known dielectric heterogeneity effects that would supplement the current approach.<sup>11,26</sup> The two polymers interact via short-range interactions using a Flory–Huggins  $\chi$ -parameter.<sup>3</sup> We write the Hamiltonian  $\tilde{\mathcal{H}}_{\text{RPA-LS}}$  for this system<sup>14</sup>

$$\begin{aligned} \tilde{\mathcal{H}}_{\text{RPA-LS}} = & \frac{1}{\nu_0} \chi \int d\mathbf{x} \phi_A \phi_B - \frac{1}{\nu_0} \int d\mathbf{x} [\tilde{\omega}_A \phi_A + \tilde{\omega}_B \phi_B] \\ & + \frac{\tilde{\eta}}{\nu_0} \int d\mathbf{x} (1 - \phi_A - \phi_B) - n_A \ln Q_A[\tilde{\omega}_A^*] \\ & - n_B \ln Q_B[\tilde{\omega}_B] \end{aligned} \quad (1)$$

The functionals  $Q_A$  and  $Q_B$  are the single-chain partition functions ( $Q_X[\tilde{\omega}_X] = V^{-1} \int q(\mathbf{x}; N) d\mathbf{x}$ , where  $\partial q(\mathbf{x}; s)/\partial s = [b^2 \nabla^2/6 - \tilde{\omega}_X] q(\mathbf{x}; s)$  and  $q(\mathbf{x}; 0) = 1.0$ ).<sup>4</sup> The parameter  $\tilde{\eta}$  is a Lagrange multiplier that sets the constraint that  $\phi_A + \phi_B = 1.0$ , and the fields  $\omega_A$  and  $\omega_B$  are internally generated fields that are conjugate to the densities  $\phi_A$  and  $\phi_B$ , respectively.<sup>4</sup> Tildes denote normalization by  $k_B T$ .  $\tilde{\omega}_A^* = \tilde{\omega}_A + f_q \tilde{\mu}_C$  is denoted with an asterisk due to the inclusion of the value  $\tilde{\mu}_C$  which is the excess potential that represents the effect of local charge structure; in our case  $\tilde{\mu}_C = 2\tilde{\mu}_{\text{EXC}} + \tilde{\mu}_0$  is related to the excess chemical potential  $\tilde{\mu}_{\text{EXC}}(f_q \phi_A)$  calculated from liquid state (LS) theory and the ideal gas chemical potential  $\tilde{\mu}_0 \sim \ln f_q \phi_A$ .  $\tilde{\mu}_{\text{EXC},i} = \rho_i/2 \int dr h_{ij}(h_{ij} - c_{ij}) - \rho_j \int dr c_{ij}$  is calculated using the functions  $h_{ij}(r)$  and  $c_{ij}(r)$  that are the total and direct correlation functions, respectively, between species  $i$  and  $j$ .<sup>28</sup> These are calculated using the numerical solution of the Ornstein–Zernike equation  $\hat{h}_{ij} = \hat{c}_{ij} + \rho_k \hat{c}_{ik} \hat{h}_{kj}$  ( $\rho_k$  is the charge density of species  $k$ , hats denote Fourier-transformed values)<sup>28</sup> and the DHMSA closure (see eqs 6–8 of Zwanikken et al.<sup>29</sup>).  $\tilde{\mu}_C$  is therefore a function of  $\phi_A$  since the charge density  $\rho_k \sim \phi_A$  is an input into its determination.<sup>14,28</sup> Calculations using this Hamiltonian reproduce features on a polymer length scale and charge ordering length scale simultaneously, which contrasts to previous approaches that do not capture charge correlations.<sup>14</sup> This implicit inclusion of the charge-based field  $\mu_C$  permits the use of complicated forms that rely on both the charge and uncharged structural features. Specifically, we can use  $\mu_C$  calculated via LS theory to take into account the local charge structures that are manifestations of the higher-order terms that are poorly represented in traditional RPA of electrolyte systems.<sup>14,27,28</sup> By including this field that represents local structure, we therefore include the appropriate information such that the charges are treated with nearly complete correlation information.<sup>14</sup> We refer to previous works by the authors that discuss in detail the use of this Hamiltonian in the context of self-consistent field theory (SCFT) calculations.<sup>14,15</sup>

It is possible to expand this Hamiltonian for a polyelectrolyte blend to the second order and subsequently evaluate the partition function in a way that accounts for fluctuations at the Gaussian level. We note that we limit ourselves to the case of a blend, which is known to be well-described by RPA in the limit of  $N \rightarrow \infty$ .<sup>30</sup> While previous works using this theory have investigated block copolymers,<sup>16</sup> RPA and similar approaches are highly nontrivial even for diblock copolymers due to the contributions of higher-order perturbation terms.<sup>19</sup> While such calculations have been carried out for certain systems, such as random polyampholytes,<sup>20</sup> it is unclear how to do so upon inclusion of charge in the current framework. Nevertheless, even with the case of the polyelectrolyte blend we can develop an understanding of the role of charge correlations in

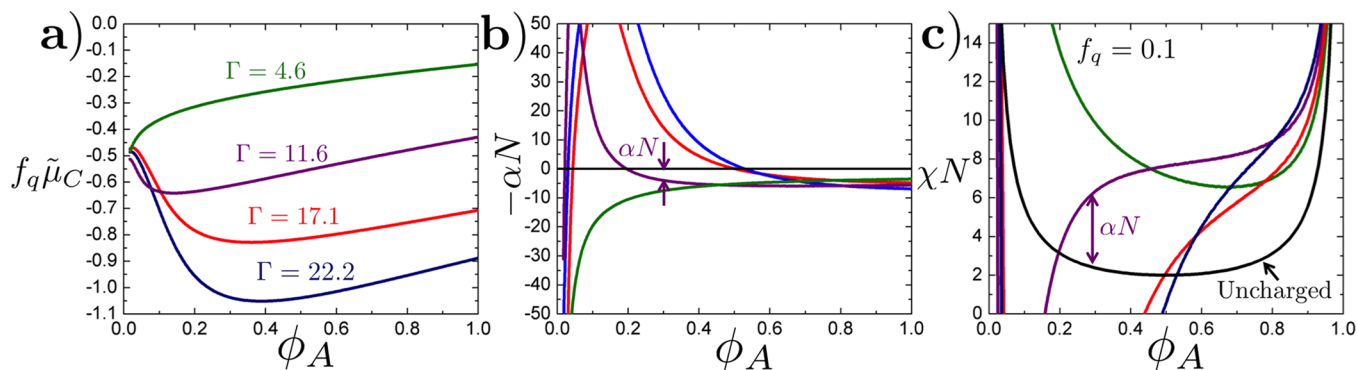


**Figure 2.** (a) Examples of curves for  $f_q \tilde{\mu}_C$  that represent the combined potential of the backbone and counterion charges as a function of  $\phi_A$  and  $\Gamma$ .<sup>31</sup> LS theory is used to calculate these trends with  $f_q = 0.1$ . Nonmonotonic trends are observed when  $\Gamma$  is large (i.e., when charge correlations are pronounced). The slope  $\alpha_1$  and curvature  $\alpha_2$  combine to produce the parameter  $\alpha$  given in eq 9; this  $-\alpha N$  term is shown in (b) for the same cases shown in (a). When  $-\alpha N > 0$ ,  $\chi_{\text{eff}} > \chi$  is observed, and phase separation is enhanced. Conversely, when  $-\alpha < 0$  then  $\chi_{\text{eff}} < \chi$  and phase separation is suppressed. Use of this correction term yields the calculations shown in (c) for the spinodals of the same systems shown in (a) and (b). Purple arrows in (b) and (c) demonstrate how  $\alpha$  dictates the charge-based shift of the phase diagram away from the uncharged spinodal.

manipulating the observed  $\chi_{\text{eff}}$ . We replace the fields  $\omega$  and  $\phi$  by their deviations from a homogeneous state (for example,  $\tilde{\omega}_B(\mathbf{x}) \rightarrow \langle \tilde{\omega}_B \rangle + \delta \tilde{\omega}_B(\mathbf{x})$ ). Importantly, we also include the consideration that the variations in the fields  $\tilde{\omega}_A^*$  include the excess chemical potential  $\tilde{\mu}_C$  that is dependent on local electrostatic conditions. Correspondingly,  $\tilde{\mu}_C = \tilde{\mu}_C(\phi_A)$  is a function of  $\phi_A$ , which is one of the other fields over which we are perturbing. Therefore, we incorporate the replacement  $\delta \tilde{\omega}_A^* \rightarrow \delta \tilde{\omega}_A + \alpha_1 \delta \phi_A + (1/2) \alpha_2 \delta \phi_A^2$  where we define the values  $\alpha_1 = f_q (\partial \tilde{\mu}_C / \partial \phi_A)$  and  $\alpha_2 = f_q (\partial^2 \tilde{\mu}_C / \partial \phi_A^2)$ . We can define the zeroth-order contribution to the Hamiltonian  $\tilde{\mathcal{H}}_{\text{RPA-LS},0}$ :

$$\begin{aligned} \tilde{\mathcal{H}}_{\text{RPA-LS},0} = & \frac{V}{\nu_0} [\chi \langle \phi_A \rangle \langle \phi_B \rangle - \langle \tilde{\omega}_A \rangle \langle \phi_A \rangle + \langle \tilde{\omega}_A^* \rangle \langle \phi_A \rangle \\ & + \tilde{\eta} (1 - \langle \phi_A \rangle - \langle \phi_B \rangle)] \end{aligned} \quad (2)$$

where we have made the replacement  $n_A \ln Q[\langle \tilde{\omega}_A^* \rangle] = V \langle \phi_A \rangle \langle \tilde{\omega}_A^* \rangle / \nu_0$  (and the same for B).<sup>4</sup> Upon replacing perturbations by their Fourier modes,  $\delta \Phi(\mathbf{x}) = (1/V) \sum_{\mathbf{k}} \delta \hat{\Phi}(\mathbf{k}) e^{-i\mathbf{k}\cdot\mathbf{x}}$  (where  $\Phi = \omega_A, \omega_B, \phi_A$ , or  $\phi_B$ ), we can write the second-order contribution to  $\tilde{\mathcal{H}}_{\text{RPA-LS}}$  as

$$\begin{aligned} \tilde{\mathcal{H}}_{\text{RPA-LS},2} = & \frac{1}{V\nu_0} \sum_{\mathbf{k}} \left[ \chi \delta \hat{\phi}_A(\mathbf{k}) \delta \hat{\phi}_B(-\mathbf{k}) - \frac{1}{2} \alpha_2 \langle \phi_A \rangle \delta \hat{\phi}_A(\mathbf{k}) \delta \hat{\phi}_A(-\mathbf{k}) \right. \\ & - \delta \tilde{\omega}_A^*(\mathbf{k}) \delta \hat{\phi}_A(-\mathbf{k}) - \delta \tilde{\omega}_B(\mathbf{k}) \delta \hat{\phi}_B(-\mathbf{k}) \\ & - N_A \frac{\phi_A}{2} g_D(k^2 R_G^2) \delta \tilde{\omega}_A^*(\mathbf{k}) \delta \tilde{\omega}_A^*(-\mathbf{k}) - N_B \frac{\phi_B}{2} g_D(k^2 R_G^2) \delta \tilde{\omega}_B(\mathbf{k}) \\ & \left. \delta \tilde{\omega}_B(-\mathbf{k}) \right] \end{aligned} \quad (3)$$

where  $g_D(m) = 2(m-1+e^m)/m^2$  is the Debye function that results from the weak inhomogeneity expansion of the partition function (derived in, e.g., ref 4)<sup>4</sup>

$$\begin{aligned} \frac{\nu_0 n_X}{V} \ln Q_X[\tilde{\omega}_X] \approx & \langle \phi_X \rangle \langle \tilde{\omega}_X \rangle - \phi_X \int d\mathbf{x} \delta \tilde{\omega}_X(\mathbf{x}) \\ & + \frac{N \phi_X}{2V^2} \sum_{\mathbf{k}} g_D(k^2 R_{G,X}^2) \delta \tilde{\omega}_X(\mathbf{k}) \delta \tilde{\omega}_X(-\mathbf{k}) \end{aligned} \quad (4)$$

While the second term of this expansion is typically zero due to the definition of the perturbation as being away from the mean value, the expansion of  $\tilde{\omega}_A^*$  out to a quadratic term leads to

$\phi_A \int d\mathbf{x} \delta \tilde{\omega}_A^* = (\phi_A/V^2) \sum_{\mathbf{k}} \alpha_2 / 2 \delta \hat{\phi}_A(\mathbf{k}) \delta \hat{\phi}_A(-\mathbf{k})$  which is the second term on the right side of eq 3. Using this expansion of the Hamiltonian,  $\tilde{\mathcal{H}}_{\text{RPA-LS}} \approx \tilde{\mathcal{H}}_{\text{RPA-LS},0} + \tilde{\mathcal{H}}_{\text{RPA-LS},2}$ , we can evaluate the resulting partition function  $Z$  due to the transformation to a Gaussian integral

$$\begin{aligned} Z \sim & e^{-\tilde{\mathcal{H}}_{\text{RPA-LS},0}} \int \mathcal{D}\delta\phi_A \mathcal{D}\delta\phi_B \mathcal{D}\delta\omega_A \mathcal{D}\delta\omega_B \\ & e^{-\tilde{\mathcal{H}}_{\text{RPA-LS},2}[\delta\phi_A, \delta\phi_B, \delta\omega_A, \delta\omega_B]} \end{aligned} \quad (5)$$

Upon integrating over every field except for  $\delta\phi_A$ , we obtain an equation of the form

$$Z \sim e^{-\tilde{\mathcal{H}}_{\text{RPA-LS},0}} \int \mathcal{D}\delta\hat{\phi}_A e^{-1/2V\nu_0 \sum_{\mathbf{k}} S^{-1}(\mathbf{k}) \delta \hat{\phi}_A(\mathbf{k}) \delta \hat{\phi}_A(-\mathbf{k})} \quad (6)$$

where the quantity  $S^{-1}(\mathbf{k})$  is the inverse scattering function (see Appendix B of ref 26 for a description of this process).<sup>26</sup> When  $S^{-1}(0) = 0$ , long-wavelength fluctuations become unstable, which represents the spinodal curve.<sup>18</sup> For a polyelectrolyte blend, we obtain the result

$$S^{-1}(\mathbf{k}) = \frac{1}{g_D(k^2 R_G^2) N \phi_A} + \frac{1}{g_D(k^2 R_G^2) N \phi_B} - 2\chi - \langle \phi_A \rangle \alpha_2 + 2\alpha_1 \quad (7)$$

This result yields insight into the overall behavior of a polyelectrolyte blend in relationship to the behavior of an uncharged blend via a straightforward mapping. The well-known value of  $S_{\text{uncharged}}^{-1}$  for an uncharged system is<sup>18,30</sup>

$$S_{\text{uncharged}}^{-1}(\mathbf{k}) = \frac{1}{g_D(k^2 R_G^2) N \phi_A} + \frac{1}{g_D(k^2 R_G^2) N \phi_B} - 2\chi \quad (8)$$

This leads to the general expression for a charged blend in the limit of  $N \rightarrow \infty$  (i.e., higher-order terms become negligible)

$$\chi_{\text{eff}} = \chi - \alpha(\phi_A, \Gamma, f_q) \quad (9)$$

where  $\alpha = \alpha_1 - \langle \phi \rangle \alpha_2 / 2$ . This is deceptively simple. While the correction term  $\alpha$  contains only the unknowns  $\alpha_1$  and  $\alpha_2$ , determining its functional form and even understanding its physical basis require the elucidation of the local thermodynamic information that describes the ordered, charged components. These local charged data are dependent on the volume fraction  $\phi_A$ , the magnitude of charge interactions  $\Gamma$ , and

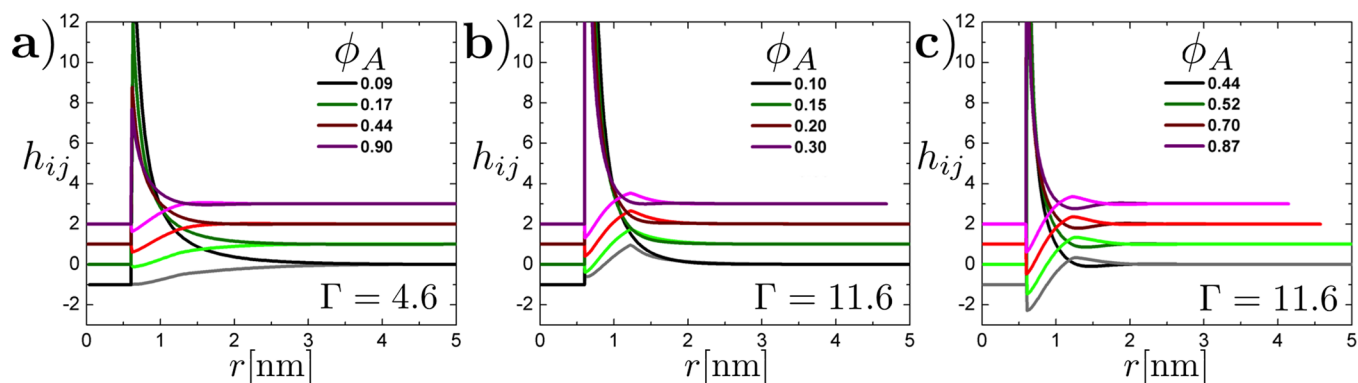


**Figure 3.** (a) Correlation functions  $h_{ij}(r)$  for charges at a number of values  $\phi_A$  in systems with  $\Gamma = 4.6$ . As  $\phi_A$  increases, correlations become less pronounced; charge structure is typical of weakly coupled Coulombic systems with charges surrounded by an abundance of the opposite charge (i.e., minimal charge ordering). (b) Strengthening the Coulombic coupling ( $\Gamma = 11.6$ ) leads to enhanced charge ordering and at low  $\phi_A$  the formation of oscillatory  $h_{ij}$  where a like-charge peak appears at ca. 1.3 nm as  $\phi_A$  is increased to  $\phi_A \approx 0.2$ – $0.3$ . This change in the correlation behavior is related to the initial decrease in  $\tilde{\mu}_C$  seen in Figure 2a that corresponds to an enhancement in  $\chi_{\text{eff}}$ . (c) At larger values of  $\phi_A$  for  $\Gamma = 11.6$  structural features do not change drastically, leading to  $\tilde{\mu}_C$  behaving similarly in both  $\Gamma = 4.6$  and  $11.6$  in Figure 2a (and correspondingly similar values of  $\alpha$  at high  $\phi_A$  in Figure 2b). For all graphs of  $h_{ij}$ , lighter colors are  $i = j$ ; darker colors are  $i \neq j$ ; and graphs are offset by 1 for clarity.<sup>32</sup>

the charge fraction  $f_q$ , and therefore  $\chi_{\text{eff}}$  changes as the phase diagram is traversed from left to right.

It is possible to calculate the function  $\mu_C$  as a function of  $\phi_A$ ,  $f_q$ , and  $\Gamma$ . We graph a few examples of such a curve in Figure 2a, which plots  $\tilde{\mu}_C$  versus  $\phi_A$  for  $f_q = 0.1$  and  $\Gamma = 4.6$ – $22.2$ .<sup>14</sup> It is the slope  $\alpha_1$  and curvature  $\alpha_2$  of Figure 2a that contribute to the value of  $\chi_{\text{eff}}$  via eq 9. This correction  $-\alpha N$  is plotted for the same conditions in Figure 2b, which demonstrates that  $\chi_{\text{eff}}$  changes drastically as a function of  $\phi_A$  and is highly nonmonotonic. The results of this mapping are demonstrated in Figure 2c which plots the corresponding spinodal curves for a blend with  $N = 40$  and  $f_q = 0.10$ . Also plotted is an uncharged blend, which follows the spinodal given by eq 8. The results of this stability analysis shown in Figure 2 match well to previous SCFT–LS results in the literature.<sup>15</sup>

The parameter  $\alpha$  is partly a representation of local structural changes, which can be demonstrated upon considering the correlation functions  $h_{ij}(r)$  calculated from LS theory. As an example, we contrast the behavior of a weakly coupled system and a more strongly coupled system. Figure 3a demonstrates  $h_{ij}(r)$  as  $\phi_A$  is increased over the range  $\phi_A = 0.09$ – $0.90$  for  $\Gamma = 4.6$  (weakly coupled). In this case there is an abundance of opposite charges in a disperse area around a given charge; this correlation decreases as  $\phi_A$  increases. Alternatively, Figure 3b shows that an increase in  $\phi_A$  for  $\Gamma = 11.6$  initially results in enhanced ordering of the system. This is characterized by the appearance of oscillatory features in  $h_{ij}(r)$  that correspond to the appearance of a local excess of correlated like charges beyond the immediately adjacent opposite charges. The formation of this order represents a drastic change in the excess chemical potential since the local correlation environment of each incorporated charge likewise changes. Furthermore, the increased magnitude of Coulombic interactions (due to the larger value of  $\Gamma$ ) enhances the magnitude of this change in  $\tilde{\mu}_C$ . This structural change is the basis of  $\alpha$  and corresponds directly to the initial decrease of  $\tilde{\mu}_C$  in Figure 2a. As  $\phi_A$  is further increased for  $\Gamma = 11.6$ ,  $h(r)$  does not show drastic correlation changes (Figure 3c), and the behavior of  $\tilde{\mu}_C$  becomes similar between  $\Gamma = 4.6$  and  $11.6$  (see high- $\phi_A$  regions in Figure 2a). In this regime ion entropy (translational and excluded volume) effects dominate  $\alpha$  since Coulombic correlations remain roughly constant. This change in balance

between ion entropy and Coulombic correlations drives the nonmonotonicity in  $\alpha$  seen in Figure 2b.

We have only calculated the perturbations around a homogeneous state, and thus the RPA result is strictly applicable in the  $N \rightarrow \infty$  limit for a disordered blend;<sup>30</sup> extensions to block copolymers are nontrivial due to the need to include higher-order terms in the perturbation expansion to describe the phase diagram appropriately.<sup>19</sup> Nevertheless, the conceptual incorporation of local charge ordering via the SCFT–LS Hamiltonian as a highly nonmonotonic contribution with dependence on both  $f_q$  and  $\phi_A$  suggests that the use of a  $\chi_{\text{eff}}$  in charged systems may obscure a rich phenomenology. Such a parameter naturally incorporates effects due to changes in local charge structure (here captured using  $\mu_C$  and its relationship to  $h(r)$ ) in a manner mathematically similar to but physically very different from the bare  $\chi$ -parameter. We note that  $\mu_C$  could be any potential field that captures local degrees of freedom; for example, the current model for  $\mu_C$  neglects chain connectivity between charges. In principle this could be incorporated via more elaborate LS-based theories;<sup>33</sup> however, upon determination of a corresponding  $\mu_C$  the treatment within RPA would be identical. Upon phase separation, the value of  $\chi_{\text{eff}}$  would become spatially varying as the system becomes far from the homogeneous state due to this  $\phi_A$  dependence. Since all of these effects are understandable in the context of the phase diagrams that we create via RPA or SCFT–LS, and since there is a pragmatism to characterizing experimental data (such as scattering data) with a  $\chi_{\text{eff}}$ , we suggest that the  $\chi_{\text{eff}}$  parameter (or perhaps rather the less confusing value  $\alpha$ ) is best interpreted as a measurement of the local charge structure upon comparison to the analogous uncharged blend of the same composition and charge fraction. This interpretation of  $\chi_{\text{eff}}$  will be especially instructive for experiments where the charge on a polymer can be systematically varied, such as in poly(ethylene oxide)/lithium salt systems commonplace in polymer electrolytes.<sup>9,10,12</sup> Observing the shift in phase diagrams of blends using this type of variably charged component would enable the probing of  $\alpha$  and correspondingly the local charge structure. Alternatively, the chemical nature of the charged species (counterion size, valency, etc.) could be tuned to alter overall phase behavior in a fashion that is predicted based on local charge structures.

In conclusion, we can use RPA and the Hamiltonian from SCFT–LS to obtain the stability criterion for a polyelectrolyte blend as a function of local structural information. This local information is incorporated into a parameter  $\alpha$  that is related to the experimentally accessible value  $\chi_{\text{eff}}^{7,9,11,12}$ . The complicated phenomenology of this term suggests that using a  $\chi_{\text{eff}}$  term is only useful if the full extent of the caveats surrounding it is understood; unlike the traditional  $\chi$  it is not related to a simple second virial coefficient of the free energy but a term that changes as the local charge densities change. Furthermore, the current calculation only considers blends, and it is not clear if this correction is transferrable to more elaborate systems (e.g., block copolymers). Nevertheless, the underlying physics is of practical importance due to the widespread parametrization of scattering curves with  $\chi_{\text{eff}}^{12}$  and this theory would inform the conceptual understanding of such results in the context of systems with large amounts of local order.

## AUTHOR INFORMATION

### Corresponding Author

\*E-mail: m-olvera@northwestern.edu.

### Notes

The authors declare no competing financial interest.

## ACKNOWLEDGMENTS

The authors acknowledge support from NSF grant number DMR-1309027. CES thanks the Northwestern International Institute for Nanotechnology for an International Institute for Nanotechnology Postdoctoral Fellowship. The computational cluster is funded by the Office of the Director of Defense Research and Engineering (DDR&E) and the Air Force Office of Scientific Research (AFOSR) under Award no. FA9550-10-1-0167.

## REFERENCES

- (1) Huggins, M. J. *Phys. Chem.* **1942**, *46*, 151.
- (2) Flory, P. J. *J. Chem. Phys.* **1942**, *10*, 51.
- (3) Flory, P. J. *Principles of Polymer Chemistry*; Cornell University Press: Ithaca, 1953.
- (4) Fredrickson, G. H. *The Equilibrium Theory of Inhomogeneous Polymers*; Clarendon Press: Oxford, 2006.
- (5) Leibler, L. *Macromolecules* **1980**, *13*, 1602.
- (6) Roe, R.-J.; Fishkis, M.; Chang, J. C. *Macromolecules* **1981**, *14*, 1091–1103.
- (7) Zhou, N. C.; Xu, C.; Burghardt, W. R.; Composto, R. J.; Winey, K. I. *Macromolecules* **2006**, *39*, 2373–2379.
- (8) Wang, Z.-G. *J. Phys. Chem. B* **2008**, *112*, 16205–16213.
- (9) Wang, J.-Y.; Chen, W.; Russell, T. P. *Macromolecules* **2008**, *41*, 4904–4907.
- (10) Wanakule, N. S.; Virgili, J. M.; Teran, A. A.; Wang, Z.-G.; Balsara, N. P. *Macromolecules* **2010**, *43*, 8282–8289.
- (11) Nakamura, I.; Balsara, N. P.; Wang, Z.-G. *Phys. Rev. Lett.* **2011**, *107*, 198301.
- (12) Teran, A. A.; Balsara, N. P. *J. Phys. Chem. B* **2014**, *118*, 4–17.
- (13) Huang, J.; Tong, Z.-Z.; Zhou, B.; Xu, J.-T.; Fan, Z.-Q. *Polymer* **2013**, *54*, 3098–3106.
- (14) Sing, C. E.; Zwanikken, J. W.; Olvera de la Cruz, M. *Phys. Rev. Lett.* **2013**, *111*, 168303.
- (15) Sing, C. E.; Zwanikken, J. W.; Olvera de la Cruz, M. *ACS Macro Lett.* **2013**, *2*, 1042–1046.
- (16) Sing, C. E.; Zwanikken, J. W.; Olvera de la Cruz, M. *Nat. Mater.* **2014**, *13*, 694–698.
- (17) Hall, L. M.; Stevens, M. J.; Frischknecht, A. L. *Phys. Rev. Lett.* **2011**, *106*, 127801.
- (18) DeGennes, P. G. *Scaling Concepts in Polymer Physics*; Cornell University Press: Ithaca, 1979.
- (19) Olvera de la Cruz, M. *Phys. Rev. Lett.* **1991**, *67*, 85–88.
- (20) Dobrynin, A. V. *J. Phys. II* **1995**, *5*, 1241–1253.
- (21) Borue, V.Yu.; Erukhimovich, I.Ya. *Macromolecules* **1988**, *21*, 3240–3249.
- (22) Marko, J. F.; Rabin, Y. *Macromolecules* **1992**, *25*, 1503–1509.
- (23) Olvera de la Cruz, M.; Belloni, L.; Delsanti, M.; Dalbiez, J. P.; Spalla, O.; Drifford, M. *J. Chem. Phys.* **1995**, *103*, 5781–5791.
- (24) Shi, A.-C.; Noolandi, J. *Macromol. Theory Simul.* **1999**, *8*, 214–229.
- (25) Wang, Q.; Taniguchi, T.; Fredrickson, G. H. *J. Phys. Chem. B* **2004**, *108*, 6733–6744.
- (26) Nakamura, I.; Wang, Z.-G. *Soft Matter* **2012**, *8*, 9356–9367.
- (27) Netz, R. R.; Orland, H. *Eur. Phys. J. E* **2000**, *1*, 203–214.
- (28) Hansen, J. P.; McDonald, I. R. *Theory of Simple Liquids*, 3rd ed.; Elsevier: Boston, 2006.
- (29) Zwanikken, J. W.; Jha, P. K.; Olvera de la Cruz, M. *J. Chem. Phys.* **2011**, *135*, 064106.
- (30) Olvera de la Cruz, M.; Edwards, S. F.; Sanchez, I. C. *J. Chem. Phys.* **1988**, *89*, 1704–1708.
- (31) We parametrize the system with  $\Gamma$ , which can change with both  $a$  and  $\epsilon_r$ . For the conditions considered in this manuscript,  $\Gamma = 4.6$  represents  $a = 0.3$  nm and  $\epsilon_r = 20.0$ ;  $\Gamma = 11.6$  represents  $a = 0.3$  nm and  $\epsilon_r = 8.0$ ;  $\Gamma = 17.1$  represents  $a = 0.25$  nm and  $\epsilon_r = 6.5$ ; and  $\Gamma = 22.2$  represents  $a = 0.25$  nm and  $\epsilon_r = 5.0$ . Different choices of these values are discussed elsewhere.<sup>16</sup>
- (32)  $h_{ij} < -1$  is an unphysical artifact of the DHEMSA closure. This is thought to have little impact on the efficacy of the closure, with excellent matching to simulation correlation behaviors and thermodynamic parameters over a wide range of values.<sup>29</sup>
- (33) Scheizer, K. S.; Curro, J. G. *Phys. Rev. Lett.* **1987**, *58*, 246–249.